Research Article

Harmful Dye Adsorption via Chitosan-Lecithin-*Pleurotus eryngii* Extract Biosorbent: Kinetic Investigations

Ayfer YILDIRIM [1],* 🆔, Hilal ACAY [2] 🆔

[1]Mardin Artuklu University, Health Services Vocational School, Mardin, Türkiye; ayferyildirim@artuklu.edu.tr

[2]Mardin Artuklu University, Faculty of Health Science, Department of Nutrition and Dietetics, Mardin, Türkiye; hilalacay@gmail.com

* Corresponding author

Abstract: This study analyses the adsorption performance of nanoparticles prepared with chitosan, lecithin, and mushroom extract as a biosorbent (KLcPEE) for various dyes, including reactive orange 16 (RO16), direct yellow 50 (DY50), acid blue 25 (AB25) anionic dyes and malachite green (MG), methylene blue (MB) cationic dyes. FE-SEM and FTIR techniques were used to characterize the surface of the biosorbent. The KLcPEE biosorbent exhibited a maximal dye removal capacity of 66.77 mg/g, 63.42 mg/g, 74.33 mg/g, 83.45 mg/g, and 147.30 mg/g for 100 mg/L aqueous medium of MG, MB, RO16, DY50 and AB25, respectively. The all cationic and anionic dyes adsorption process on KLcPEE biosorbent followed the pseudo 1st order kinetic model. Overall, this study offers an ecofriendly, sustainable, biological biosorbent, and the KLcPEE exhibit considerable potential for rapid and efficient organic cationic and anionic dye adsorption in wastewater.

Keywords: Acid blue 25; direct yellow 50; malachite green; methylene blue; reactive orange 16

Kitosan-Lesitin-*Pleurotus eryngii* Özütü Biyosorbent Yoluyla Zararlı Boya Adsorpsiyonu: Kinetik Araştırmalar

Özet: Bu çalışma anyonik reaktif turuncu 16 (RO16), direkt sarı 50 (DY50), asit mavisi 25 (AB25) ve katyonik (malakit yeşili (MG), metilen mavisi (MB) gibi çeşitli boyaların kitosan, lesitin ve mantar özütü ile hazırlanan nanopartiküllü biyosorbent (KLcPEE)'in adsorpsiyon kapasitesini analiz etmektedir. Biyosorbentin yüzeyini karakterize etmek için FE-SEM ve FTIR teknikleri kullanılmıştır. KLcPEE biyosorbent, MG, MB, RO16, DY50 ve AB25'in 100 mg/L sulu ortamı için sırasıyla 66.77, 63.42, 74.33, 83.45 ve 147.30'luk maksimum boya giderme kapasitesi sergilemiştir. KLcPEE biyosorbentteki tüm katyonik ve anyonik boyaların adsorpsiyon süreci, psödo 1.ci dereceden kinetik modeliyle uyumlu olduğu gözlemlenmiştir. Genel olarak, bu çalışma çevre dostu, sürdürülebilir, biyolojik bir biyosorbent sunmakta ve KLcPEE, atık suda hızlı ve etkili organik katyonik ve anyonik boyaların adsorpsiyonu için önemli bir potansiyel sergilemektedir.

Anahtar Kelimeler: Asit mavisi 25; direkt sarı 50; malakit yeşili; metilen mavisi; reaktif turuncu 16

1. Introduction

Essential colorants called organic dyes are important ingredients used in the pharmaceutical, food, paper, printing, and textile industries. They cause significant water pollution due to their extensive industrial use and release into water bodies without being completely removed or degraded. In addition, because of the chemically stable synthetic organic dyes, they show very low biodegradability. Therefore, it is emphasized that organic dye pollution in water poses a great risk to ecological systems and the environment [1-5]. Water pollution caused by organic dyes greatly threatens the environment and living organisms. DY50 that of a synthetic diazo dye, is primarily used for cellulosic fibers, viscose, cotton, printing, and silk dyeing [5]. RO16 sulfonated, anionic and reactive azo dye is an unbiodegradable [6]. AB25 dye widely used in dyeing nylon, fiber and protein is an anionic dye that negatively affects the ecosystem because it contains organic sulphonic groups [7]. MG and MB are cationic dyes that have many harmful effects, including mutagenicity and carcinogenicity, on various organisms, especially humans and animal species, at low concentrations [8]. Releasing these dyes into the environment is dangerous, toxic and mutagenic for humans, animals and herbals. As a result, there is an increasing demand for removing toxic organic compounds such as dyes in wastewater.

Removing dyes from wastewater usually adopts coagulation, chemical precipitation, adsorption, membrane filtration, flotation, ion exchange, electrochemical methods, and flocculation. The adsorption method has become the best alternative among existing technologies when compared to other methods due to its advantages of low cost, wide application range and convenient operation. Many researchers have recently developed new and improved biocomposites including alginate-sepiolite [9], lignin-chitosan [10], chitosan-cellulose [11], chitosan-sodium alginate [12], Polyaniline@Hydroxyapatite [13], Starch-metalorganic framework-Graphene oxide [14], and Zeolite-Guar gum-Polyvinylpyrrolidone [15] to remove dyes with great adsorption capacities in the literature. In addition, new adsorbents with higher adsorption capacity and superior properties continue to be researched.

Various functional groups in the structure of nanosorbents play an active role in the formation of different dye adsorption. Chitosan, natural cationic macromolecular chains with abundant amine and hydroxyl groups, is a biocompatible, biodegradable, antibacterial biomass material, renewable, and non-toxic. These features make it the most suitable choice for the design of functional materials for applications [16-18]. Soy lecithin, a mixture of phosphatidic acid, phosphatidylcholine and phosphatidyl inositol, is a biopolymer derived from soybeans. Its emulsification tendency, antioxidant ability, high wettability properties, and biodegradable structure make this biopolymer superior [19]. Due to its excellent biocompatibility, Lecithin is widely used as an important bio-activator or natural surfactant in many industries, such as cosmetics, food and pharmaceuticals. Lecithin has a negative charge on the phosphate group and a positive charge on the trimethyl-amino group, and taking into account that the composite is both negative /positive compound, a repulsive interaction between the composite and anionic/cationic dyes should be expected. This makes the inclusion of lecithin in the composite help increase the adsorption efficiency. Mushrooms are a rich source of various carbohydrates such as chitin, mannans, hemicellulose, beta-glucans, galactans, and xylans. This content gives mushrooms a wide range of functional groups, making them a very assertive material for composite materials used in various dye adsorption. Furthermore, using the mushroom to produce composites is an ecological, sustainable and economically viable alternative, providing a residue that could become an environmental liability [18]. *Pleurotus eryngii* is an oyster mushroom that is a possible source of proteins and cell wall polysaccharides, primarily β-D-glucans. In this study, a perfect alternative composite was prepared in the literature for dye removal by creating a synergistic effect of chitosan by adding lecithin and mushroom by their functional groups.

In this study, chitosan-lecithin-*Pleurotus eringii* extract biosorbent (KLcPEE) was synthesized and the adsorption efficiency of cationic dyes: MG, MB, and anionic dyes: RO16, DY50, AB25 dyes adsorption was investigated. Figure 1 shows the chemical structure of these anionic and cationic dyes. The adsorption experiments were conducted using, temperature, pH, the concentration of initial dye and contact time. Kinetic models called Pseudo 1st order and pseudo 2nd order to investigate the adsorption kinetics.
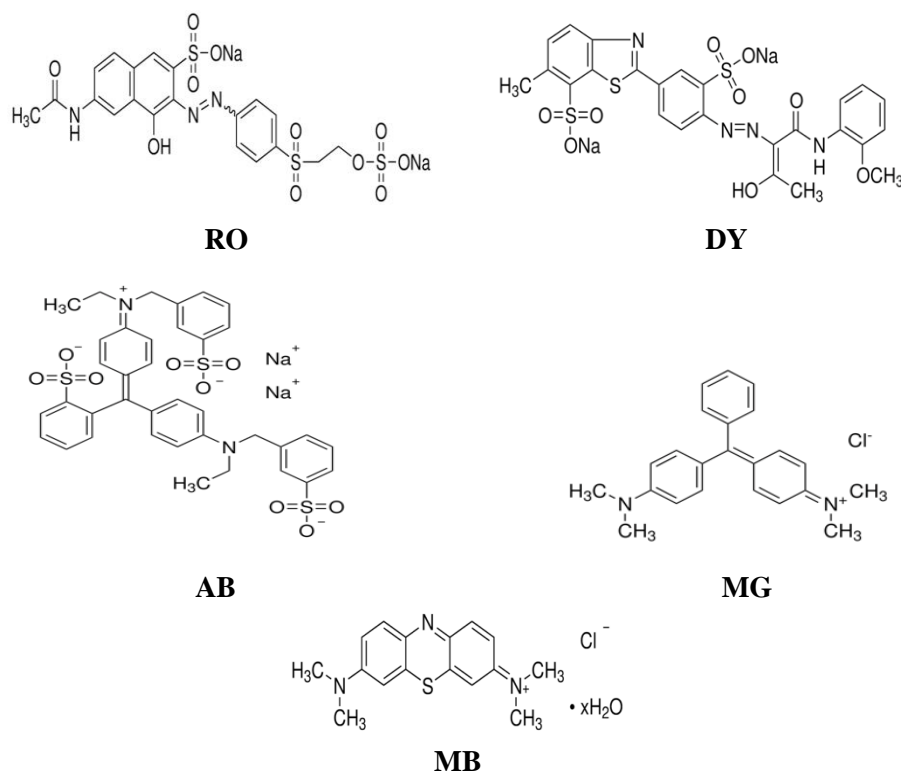
Figure 1. Schematic illustration of anionic (RO, DY, AB) and cationic (MG, MB) dyes

2. Materials and Methods

Low-density chitosan (K) and lecithin (Lc) were produced from Sigma-Aldrich production. *Pleurotus eringii* extract (PEE) was prepared using our previous procedure [17]. FTIR spectroscopy was used to examine the chemical composition of the KLcPEE biosorbent. Bruker Spectrometer, (ALPHA) (with ZnSe crystal and a Platinum-ATR accessory) instrument was used to investigate the functional groups onto biosorbent. device of EVO-40 LEQ 20 kV unit energy was used to determine the surface morphology of KLcPEE biosorbent.

2.1. Synthesis of KLcPEE

0.50 g K was dissolved in 30 mL 1% acetic acid solution and pH was adjusted to ≈ 5.6. Then, 0.05 g tripolyphosphate (TTP) was dissolved in 15 mL distilled water and the solution was stirred again. In addition, 1.5 g Lc was dissolved in 70 mL distilled water while 0.060 g PEE was dissolved in methanol, and both solutions were added to K-TTP (pH≈5.5) solution and the mixture was stirred 4-5 h by magnetic stirring apparatus. After stirring, the mixture was centrifuged and dried at 323 K. Finally, the nanosorbent was sieved and used for further experiments.

2.2. Adsorption Experiments and Kinetics

For adsorption experiments, first of all, for examination of the effect of initial dye concentration and contact time, experimental conditions as the adsorbent amount (m): 0.01 g, dye volume (V): 20 mL, temperature (T): 298 K, stirring speed (r):160 rpm were provided. Additionally, for kinetic studies, three different temperatures of 298 K, 303 K and 313 K were studied under the same conditions. The capacity of adsorption was calculated as below formula (2.1).

$$q = \frac{C_o - C_t}{m} * V \tag{2.1}$$

While q, mg/g, represents the capacity of adsorption, m, g, the amount of biosorbent, C_o, mg/L, is the dye's initial concentration and C_t, mg/L, is the dye concentration at t time.

Pseudo 1st order and pseudo 2nd order model equations, widely preferred in the literature, were used to investigate the adsorption kinetic parameters. The pseudo 1st order equation is as equation (2.2) [19].

$$\log(q_e - q_t) = logq_e - K_1 . \frac{t}{2.303} \tag{2.2}$$

The pseudo 2nd order equation is given by equation (2.3) [20].

$$\frac{t}{q_t} = \frac{t}{q_e} + \frac{1}{q_e^2 K_2} \tag{2.3}$$

q_e (at equilibrium, mg/g) and q_t (at t time, mg/g) represent the dye amount adsorbed on the biosorbent, while K_1 (1/min) and K_2 (g/mg.min) perform the pseudo 1st order and pseudo 2nd order rate constants, respectively.
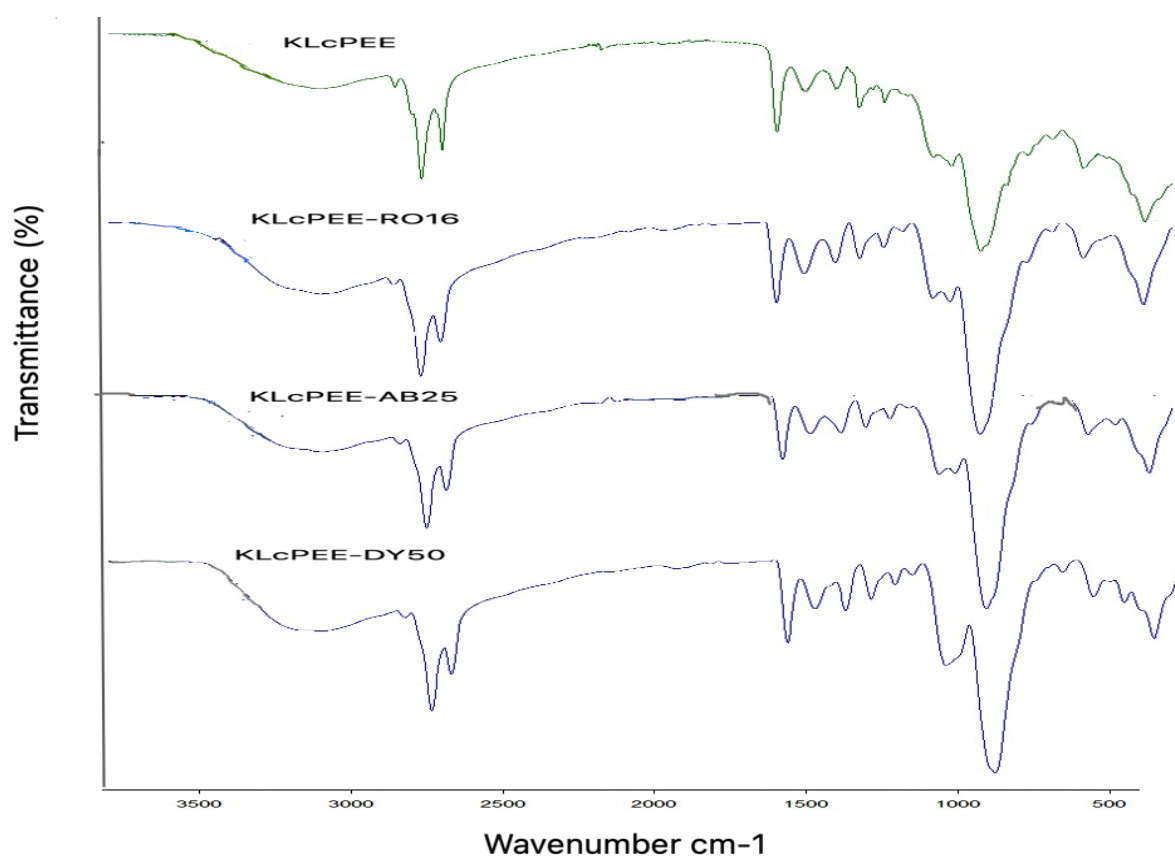
3. Results and Discussions

3.1. Characterizations
To examine the KLcPEE's chemical composition, FTIR spectroscopy was examined.
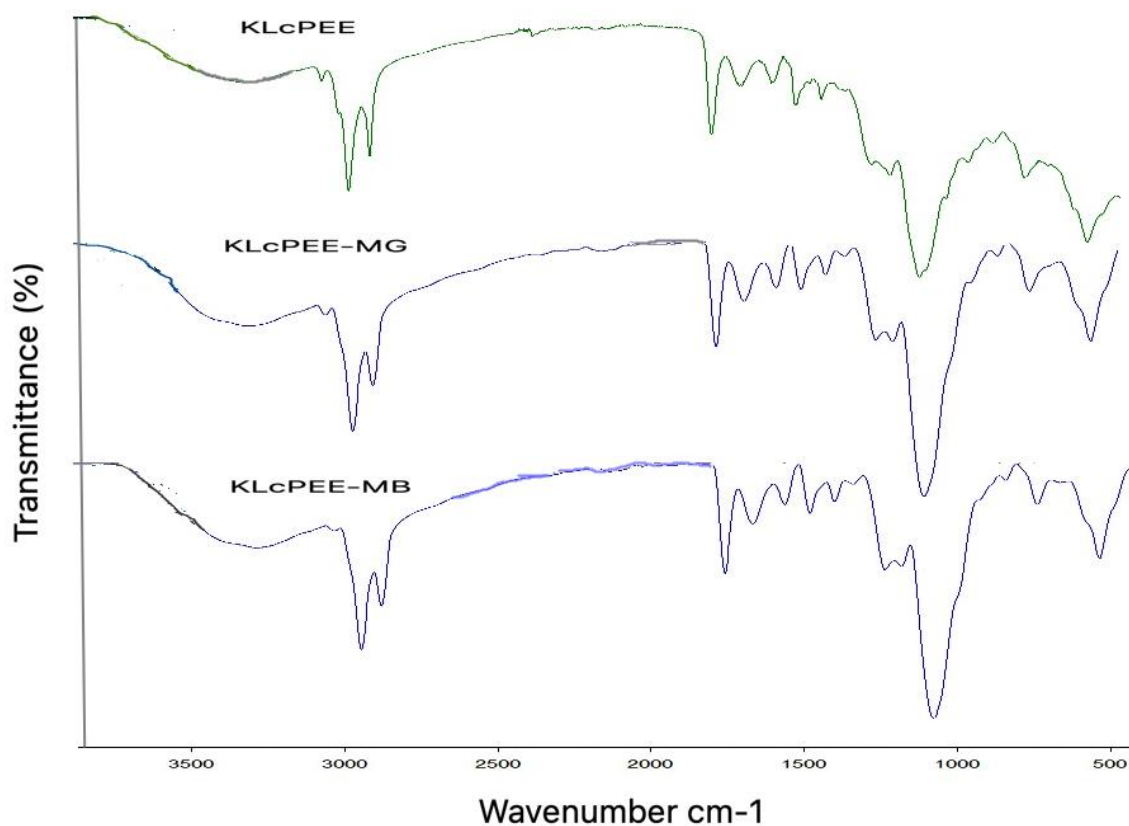
a

b

Figure 2. FTIR Spectra of KLcPEE before and after (a) cationic dyes and (b) anionic dyes

As represented in Figure 2.a, b, the peaks observed in the FTIR spectrum of KLcPEE were found to be at 3250 cm^{-1}, 2920 cm^{-1}, 2854 cm^{-1}, 1733 cm^{-1}, 1642 cm^{-1}, 1537 cm^{-1}, 1458 cm^{-1}, 1376 cm^{-1}, and 1032 cm^{-1}. The peak that appeared at 3250 cm^{-1} corresponds to the typical O-H vibration of stretching while the peaks at 2854 cm^{-1} and 2920 cm^{-1} CH$_2$ vibration of stretching [21,22]. Also, 1733 cm^{-1}, 1642 cm^{-1} and 1538 cm^{-1} peaks show carbonyl, amide I, and amide II stretching vibration, respectively. 1458 cm^{-1}, 1376 cm^{-1}, and 1032 cm^{-1} peaks are belongs to the Ar(C=C), C-N, C-O stretching vibration, respectively.

After adsorption of cationic dyes, some changes were found in the biosorbent's FTIR spectrum (Figure 2a). The peaks at 3279 cm^{-1}, cm^{-1}, 1642 cm^{-1}, 1537 cm^{-1} were sharper and shifted to 3264 cm^{-1}1, 1641 cm^{-1}, 1538 cm^{-1} and 3260 cm^{-1}, 1643 cm^{-1}, 1536 cm^{-1} after MB and MG adsorption, respectively. Also, after the adsorption of MB and MG, the peak at 1032 cm^{-1} was sharper and shifted to 1045 cm^{-1}, 1057 cm^{-1}. These changes and shiftings result from the dye molecules on the KLcPEE's surface. In addition, because of the changes that occurred at these peaks, it can be interpreted that the adsorption mechanism happened at the O-H(N-H), C=O(NH), (O=C)-NH, and C-O functional groups.

After anionic dyes (RO16, DY50, AB25) adsorption, some changes occurred again at the FTIR spectrum (Figure 2b). The peak at the 3279 cm^{-1} and 1736 cm^{-1} were shifted to 3250 cm^{-1}, 1733 cm^{-1}, 3241 cm^{-1}, 1734 cm^{-1}, 3274 cm^{-1}, 1733 cm^{-1} after RO16, DY50 and AB25 adsorption, respectively that explain the adsorption took place onto functional groups, C=O and O-H(N-H).

In addition, the new peak at the 617 cm^{-1}, 613 cm^{-1} and 629 cm^{-1} that belongs to the symmetrical vibration of SO4^{2-} (from anionic dyes) occurred after RO16, DY50 and AB25 adsorption that proved the existence of these dyes onto biosorbent. Also, after all the anionic dye, the peak at around $\approx$1000-1100 (S-O stretching of sulphate) became sharper, which also proves the RO16, DY50 and AB25 dyes onto the KLcPEE surface.

The SEM image used to identify the morphology of synthesized KLcPEE is shown in Figure 3. It revealed that the synthesized biosorbent had a roughly spherical form with a rough, highly porous inward surface. This shows that KLcPEE material is quite suitable for the adsorption of dye molecules.
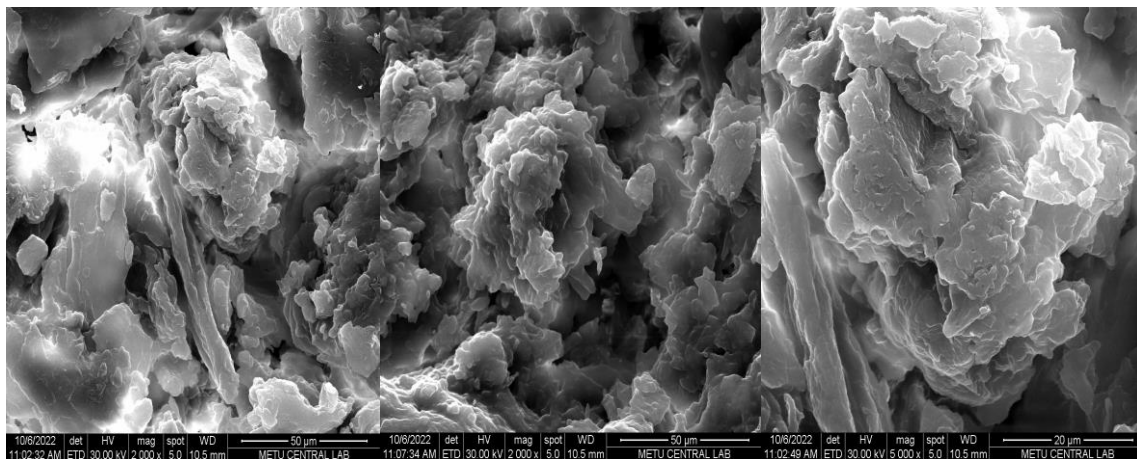

Figure 3. SEM images of KLcPEE biosorbent

3.2. Effect of Contact Time and Initial Dye

The contact time was investigated for the adsorption of MG, MB, RO16, DY50 and AB25. Initial dye concentrations of dyes, C_o:25 mg/L, 50 mg/L and 100 mg/L were selected for the dyes used in this study. For removal efficiency, the contact time of biosorbent was used as 15, 30, 60, 90, 120, 150, 180 and 240 min. As seen in Figure 4a-e, the equilibrium contact time for MG, and MB dyes was 90 min, while it was determined as 120 min for RO16, DY50 and AB25 dyes. When the adsorption efficiencies at equilibrium were examined, the highest adsorption efficiency was found to be 147.30 mg/g in AB25 dye. Other dye yields are given as follows: the adsorption efficiency was 66.77 mg/g, 63.42 mg/g, 74.33 mg/g, 83.45 mg/g and 147.30 mg/g per minute in MG, MB, RO16, DY50 and AB25 dye, respectively (Figure 4a-e).

The 25, 50 and 100 mg/L concentrations were selected for studying the effect of access on adsorption. Figure 4a-e shows the results, including the change of adsorption capacities of MG, MB, RO16, DY50 and AB25 dyes with different initial concentrations with time. As can be understood from Figure 4a-e, it is obvious that the actual dye adsorption capacities are higher at higher dye concentrations (from 25 mg/g to 100 mg/g). A high solute/adsorbent vacancy ratio at low dye concentrations promotes colour removal. As the concentration increases, the number of active adsorbate molecules to be adsorbed in the medium increases, thus, the adsorption amount also increases in parallel [23].
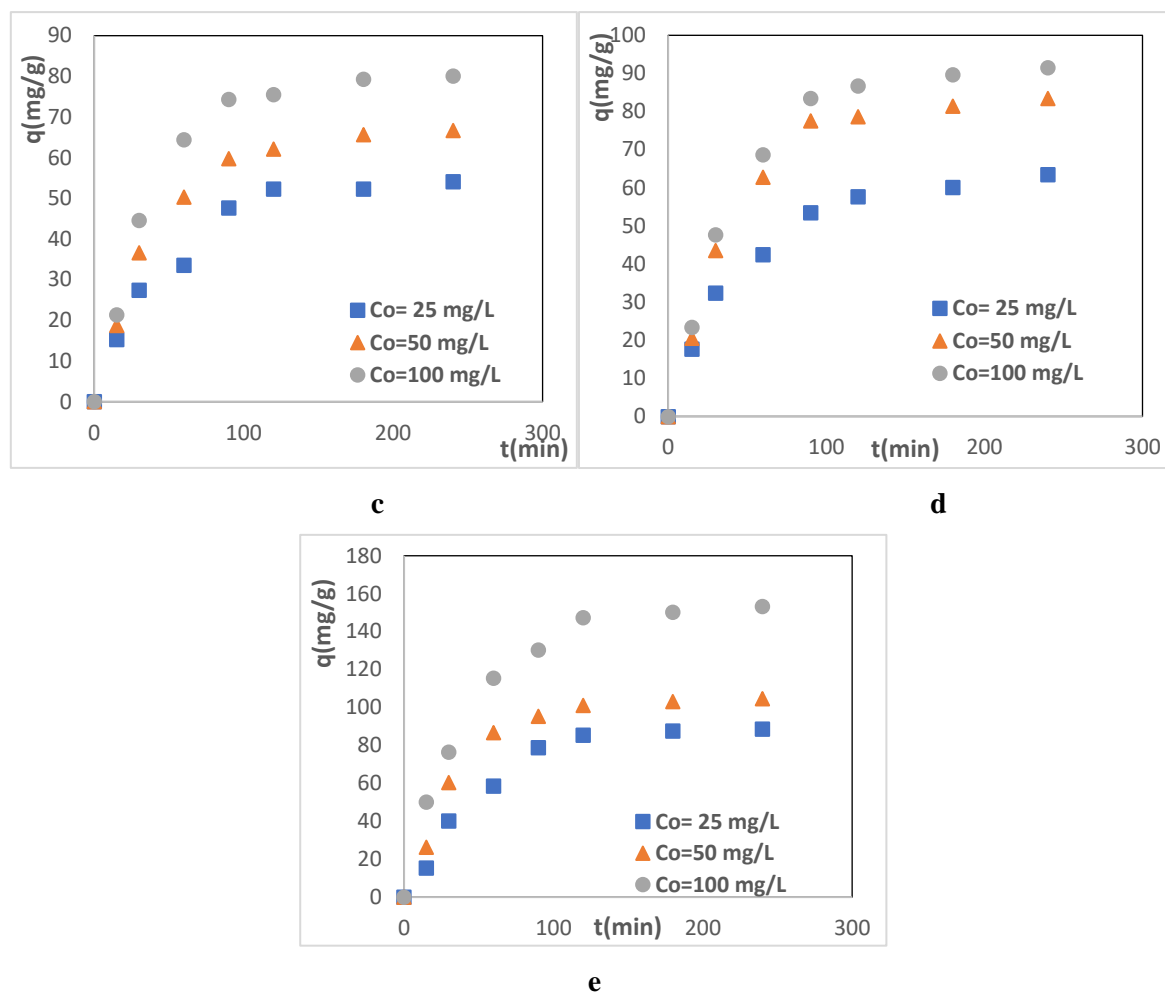

a   b
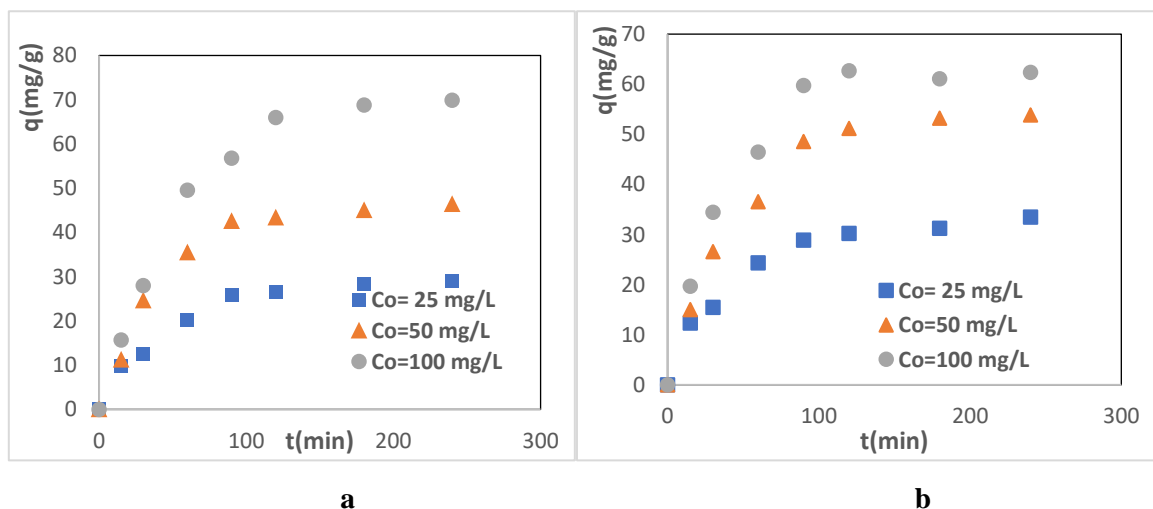
Figure 4. Initial dye concentration effect of a: MG, b: MB, c: RO16, d: DY50, e: AB25 adsorption onto KLcPEE

3.3. Kinetics of Adsorption

The data belonging to the experiments were analyzed with the pseudo 1st order (Figure 5a) and pseudo 2nd order kinetics models' plots (Figure 5b) using equations (2) and (3) for the adsorption kinetics of dyes MG, MB, RO16, DY50 and AB25 evaluation.

Both models' values of K_1 and K_2, the rate constants, the q_e, calculated adsorption capacities at equilibrium, and R^2, the linear correlation coefficients, are listed in Table 1. According to Table 1 data, the pseudo 1st order kinetic model showed a higher value of (R^2) than the pseudo 2nd order. R^2 were between 0.9904-0.9966 for pseudo 1st order while between 0.9692-0.9820 for pseudo 2nd order.

Also, the values of q_e obtained from the pseudo 1st order model are close to experimental q_e, suggesting all dyes adsorption onto the KLcPEE biosorbent' kinetics follow this model. In Figure 5a, in all cases, the plot $\log(q_e-q_t)$ versus t is a straight line. Thus, this linear plot shows that the experimental data demonstrate compatibility as the pseudo 1st order kinetic model and that this model is more favourable to describe the MG, MB, RO16, DY50, and AB25 dyes adsorption onto the KLcPEE biosorbent.

The pseudo 1st order kinetic model describes the physical adsorption of dyes. It also supports that the rate of adsorption is directly related to the number of voids on the adsorbent surface. In similar studies in the literature, pseudo 1st order adsorption data are also found [24].

Table 1. *Pseudo 1st order and Pseudo 2nd order kinetic parameters*

		Pseudo 1st order			Pseudo 2nd order		
Adsorbate	**q_e,exp (mg/g)**	**q_e,c (mg /g)**	**K_1(1/min)**	**R^2**	**q_e,c(mg/g)**	**K_2(g/mg min)**	**R^2**
MG	42.55	45.34	0.0306	0.9933	51.81	1.9489	0.9692
MB	48.56	47.28	0.0233	0.9946	60.61	2.1848	0.9723
RO16	59.77	61.49	0.0313	0.9966	73.53	3.0912	0.9795
DY50	77.55	81.00	0.0283	0.9952	100.00	2.4808	0.9836
AB25	101.20	110.41	0.0334	0.9904	123.46	3.5524	0.9820
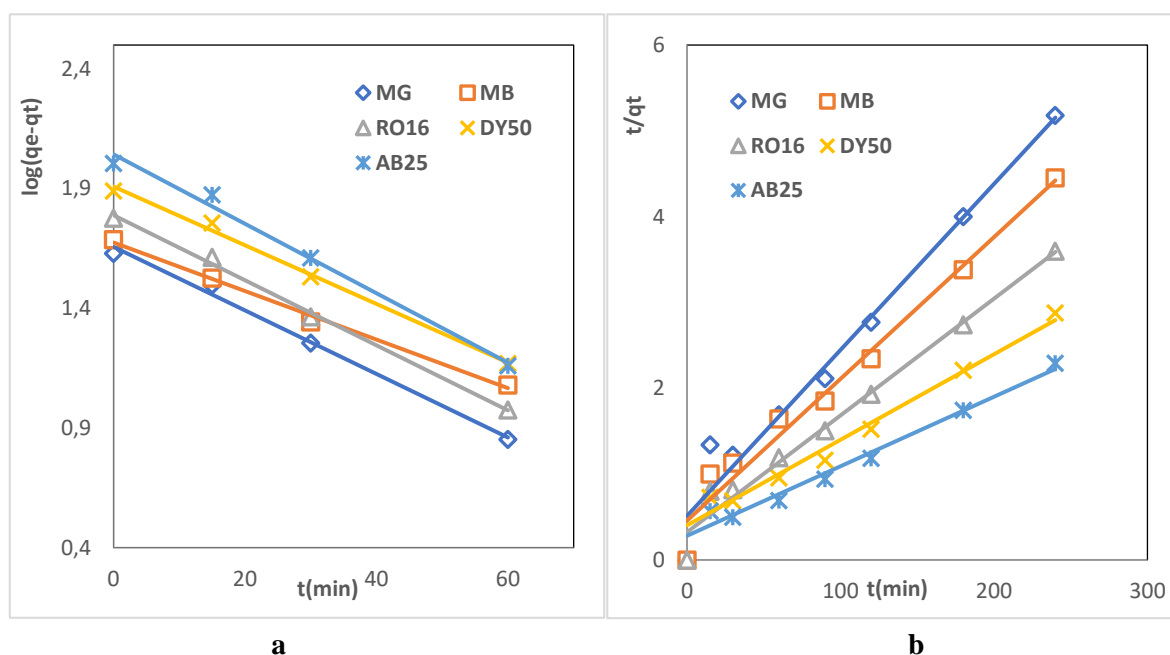
Figure 5. Kinetic plots of **a)** Pseudo 1st order **b)** Pseudo 2nd order MG, MB, RO16, DY50, AB25 onto KLcPEE

3.4. Effect of Temperature

The temperature of the solution is one of the most important factors influencing the adsorption capacity. To determine the effect of temperature on the adsorption of MG, MB, RO16, DY50, and AB25 dyes with KLcPEE, temperatures at 298 K, 303 K and 313 K were investigated with (C_o):50 mg/L, (r)=160 rpm. According to the results in Figure 6, as the rise in temperature occurs from 298 K to 313 K, the adsorption capacities for MG, MB, RO16, DY50, and AB25 dyes decrease from 42.55 mg/g to 22.68 mg/g for MG dye and from 48.56 mg/g to 25.95 mg/g for MB dye, from 60.34 mg/g to 45.76 mg/g for RO16 dye, from 78.12 mg/g to 50.53 mg/g for DY50 dye, and from 101.20 mg/g to 85.33 mg/g for AB25 dye. The decrease in the capacity of adsorption with temperature rise supports that the adsorption process is exothermic. As the temperature rises, the heat increases and as a result, the space between the particles on the solid biosorbent surface increases, making dye molecule adsorption difficult [25]. As a result, with a temperature rise, the adsorption capacity decreases. In the literature, other studies show that the adsorption mechanism is exothermic [26].
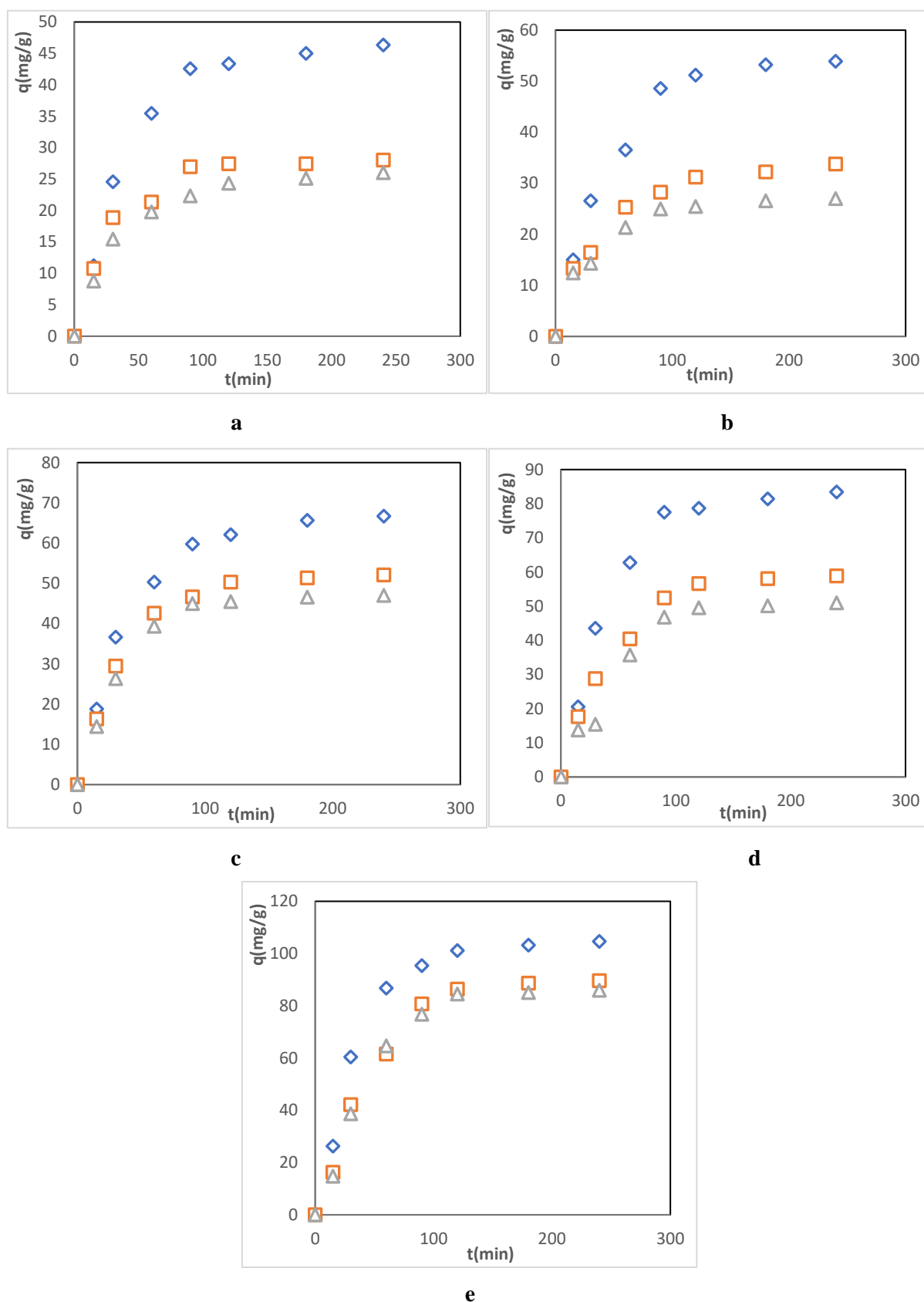
Figure 6. Temperature effect on **a**: MG, **b**: MB, **c**: RO16, **d**: DY50, **e**: AB25 adsorption onto KLcPEE (◇:298 K, • :303 K △:313 K)
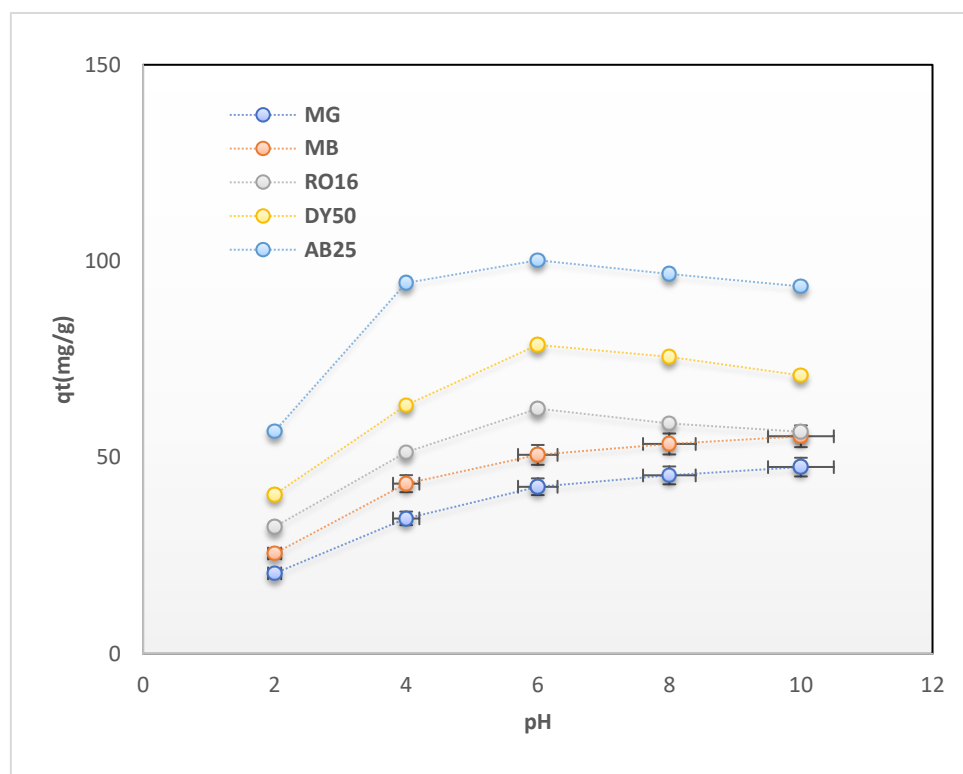
Figure 7. pH effect on **a:**MG, **b:**MB, **c:**RO16, **d:**DY50, **e:**AB25 adsorption onto KLcPEE (pH:2-10)

3.5. pH Effects on Dye Adsorption

To determine whether there is a change in the adsorption capacity levels in dye solutions of different pH environments, a study was carried out using dye solutions at C_o=50 mg/L concentration levels in the pH range of 2-10 as shown in Figure 7.

In the MG, MB cationic dyes adsorption, very little adsorption occurred at low pH, but as pH increased, the adsorption of these dyes increased (Figure 7). At low pH, the surface of the biosorbent is positively charged (protonation) and electrostatic repulsion occurs between the biosorbent's positive charge surface and the positively charged cationic dyes. However, at high pHs, the surface of the biosorbent is negatively charged (deprotonation) and attracts positively charged cationic dyes, showing a higher adsorption efficiency [27].

As seen from Figure 7 for anionic dyes, when pH increases from 2 to 7, the surface of the biosorbent is positive, so between the positively charged biosorbent surface and the anionic dye, a strong attraction of electrostatic interference occurs. With the increase of pH, both positively charged areas decrease, and the number of negatively charged areas increases, therefore, electrostatic repulsion occurs. Thus, it prevents the anions in the dyes from binding to the negatively charged areas on the surface of the biosorbent, and at higher pH levels, it further reduces the adsorption due to ionic repulsion of OH^- ions with the anionic dye molecules [28].

4. Conclusion

KLcPEE biosorbent was synthesized and used to remove MG, MB cationic dyes RO16, DY50, and AB25 anionic dyes from the aqueous solution. The effects of various factors such as temperature, pH, initial dyes' concentration and contact time were evaluated. The equilibrium time of MG and MB dyes was determined as 90 min, while that of RO16, DY50 and AB25 dyes was determined as 120 min. AB25 showed the highest adsorption capacity (147.30 mg/g, 100 mg/L) onto KLcPEE biosorbent among the dyes. Pseudo 1st order and pseudo 2nd order kinetic modelling were used in the evaluation of kinetic studies. When the correlation values (R^2) and adsorption capacities were examined, it was

determined that MG, MB, RO16, DY50, and AB25 dyes are compatible with the pseudo 1st order kinetic model. As a result, KLcPEE can be considered an effective and cost-effective adsorbent in removing both cationic and anionic dyes from wastewater.

Conflict of Interest

No conflicts of interest related to this article were declared by the authors.

Research and Publication Ethics Statement

The authors declare that this study complies with research and publication ethics.

References

[1] Xu, Z., Yang, Q., Zheng, X., Liu, X., Zhao, J., Tan, S.H., Liu, Z. (2024). All-weather-available down carbon fiber hydrogel with enhanced mechanical properties for simultaneous efficient clean water generation and dye adsorption from dye wastewater. *Journal of Colloid and Interface Science*, 669, 864-876.

[2] Baran, M.F., Yildirim, A., Acay, H., Keskin, C., & Aygun, H. (2020). Adsorption performance of Bacillus licheniformis sp. bacteria isolated from the soil of the Tigris River on mercury in aqueous solutions. *International Journal of Environmental Analytical Chemistry*, 102(9), 2013–2028.

[3] Paşa, S., Demir, İ., & Aytepe, Y. (2024). Comparative Investigation of the Color Removal Efficiency of Different Mosses Species from Dye Solutions. *International Journal of Pure and Applied Sciences*, 10(1), 136-151.

[4] Tepe, Ö. (2022). Pseudomonas putida ile Üretilmiş Biyojenik Mangan Oksit Kullanarak Remazol Brilliant Blue R Giderimi. *International Journal of Pure and Applied Sciences*, 8(2), 449-459.

[5] Alabbad, E.A. (2023). Effect of Direct yellow 50 removal from an aqueous solution using nano bentonite; adsorption isotherm, kinetic analysis and also thermodynamic behaviour. *Arabian Journal of Chemistry*, 16(2), 2023, b104517.

[6] Yildirim, A. (2021). Removal of the Anionic Dye ReactiveOrange 16 by Chitosan/Tripolyphosphate/Mushroom. *Chemical Engineering & Technology*, 44(8), 1371-1381.

[7] Saheed, I.O., Oh, W.D., Suah, F.B.M. (2021). Enhanced adsorption of acid Blue-25 dye onto chitosan/porous carbon composite modified in 1-allyl-3-methyl imidazolium bromide ionic liquid. *International Journal of Biological Macromolecules*, 183, 1026-1033.

[8] Mandale, P., Kulkarni, K., Jadhav, K., Kulkarni, A., Mahajan, R. (2024). Adsorption of malachite green dye from aqueous solution on bioadsorbent as low-cost adsorbent. Materials Today: Proceedings, XX.

[9] Chinoune, K., Mekki, A., Boukoussa, B., Mokhtar, A., Sardi, A., Hachemaoui, M., Iqbal, J., Ismail, I., Abboud, M., Aboneama, W.A. (2024). Adsorption behavior of MB dye on alginate-sepiolite biocomposite beads: Adsorption, kinetics, and modeling. *Inorganic Chemistry Communications*, 165, 112558.

[10] Wang, H., Chen, C., Dai, K., Xiang, H., Kou, J., Guo, H., Ying, H., Chen, X., Wu, J. (2024). Selective adsorption of anionic dyes by a macropore magnetic lignin-chitosan adsorbent. *International Journal of Biological Macromolecules*, 269, (Part 2), 131955.

[11] Lin, J., Gao, D., Zeng, J., Li, Z., Wen, Z., Ke, F., Xia, Z., Wang, D. (2024). MXene/ZnS/chitosan-cellulose composite with Schottky heterostructure for efficient removal of anionic dyes by synergistic effect of adsorption and photocatalytic degradation. *International Journal of Biological Macromolecules*, 269 (Part 1), 131994.

[12] Yang, J., Lou, T., Wang, X. (2024). One-step fabrication of millimeter-scale hollow vesicles with chitosan /DADMAC/ sodium alginate graft copolymer for enhanced anionic dye adsorption, *International Journal of Biological Macromolecules*, 269, Part 2, 132153.

[13] Mchich, Z., Aziz, K., Kjidaa, B., Saffaj, N., Saffaj, T., Mamouni, R. (2024). Eco-friendly engineering of micro composite-based hydroxyapatite bio crystal and polyaniline for high removal of OG dye from wastewater: Adsorption mechanism and RSM@BBD optimization. *Environmental Research*, 257, 119289.

[14] Samianifard, S.M., Kalaee, M., Moradi, O, Mahmoodi, N.M., Zaarei, D. (2024). Novel biocomposite (Starch/metal–organic framework /Graphene oxide): Synthesis, characterization and visible light assisted dye degradation. *Journal of Photochemistry and Photobiology A: Chemistry*, 450, 2115417.

[15] Moradi, A., Kalaee, M., Moradi, O., Mahmoodi, N.M., Zaarei, D. (2024). Surface coated Guar gum biocomposite (Zeolite imidazolate framework (ZIF-8)-Guar gum–Polyvinylpyrrolidone) as an environmentally friendly adsorbent: Preparation, isotherm and kinetics of pollutant removal. *Journal of Molecular Structure*, 1304, 137642.

[16] Abdulhameed, A.S., Jawad, A.H., Ridwan, M., Khadiran, T., Wilson, L.D., Yaseen, Z.M. (2022). Chitosan/carbon-doped TiO2 composite for adsorption of two anionic dyes in solution and gaseous SO2 capture: experimental modeling and optimization. *Journal of Polymers and the Environment.*, 30, 4619–4636.

[17] Acay, H., Yildirim, A., Güney, İ.G., Derviş, S. (2022). *Morchella esculenta*-based chitosan bionanocomposites: Evaluation as an antifungal agent. *Journal of Food Processing and Preservation*, 46,17117.

[18] Yıldırım, A., Acay, H., Baran, A. (2021). Synthesis and characterization of molecularly imprinted composite as a novel adsorbent and competition with non-imprinting composite for removal of dye. *Journal of the Turkish Chemical Society Section A: Chemistry*, 8(2):609-22.

[19] Bo, J., B Shi, B. (2024). Performances of residues from hydrolyzed corn-cobs for the adsorption of Congo red. *Industrial Crops and Products*, 220, 119311.

[20] Tian, H., Zhu, Z., Ma, F., Li, J., Li, J., Li, Y., Yang, P. (2024). Preparation of poly (polyethylene glycol diacrylate -co- maleic anhydride) cryogels and its adsorption performance of cationic dyes. *Reactive and Functional Polymers*, 195, 105812.

[21] Sharma, G., Kumar, A., Sharma, S., Ala'a, H., Naushad, M., Ghfar, A.A. (2019). Fabrication and characterization of novel Fe°@Guar gum-crosslinked-soya lecithin nanocomposite hydrogel for photocatalytic degradation of methyl violet dye. *Separation and Purification Technology*, 211, 895–908.

[22] Wu, R., Abdulhameed, A.S., Jawad, A.H., Musa, S.A., Luna, Y.D., ALOthman, Z.A., Algburi, S. (2024). An eco-friendly chitosan-genipin/SiO2 composite for reactive orange 16 dye removal: Insights into adsorption statistical modeling and mechanism. *International Journal of Biological Macromolecules*, 270, Part 1, 132329.

[23] Abdulhameed, A.S., Khan, M. K.A., Alshahrani, H., Younes, M.K., Algburi, S. (2024). Newly developed polymer nanocomposite of chitosan-citrate/ZrO2 nanoparticles for safranin O dye adsorption: Physiochemical properties and response surface methodology. *Materials Chemistry and Physics*, 324, 129699.

[24] Yang, Q., Guo, J., Yao, Q., Zhang, S., Feng, S., Guan, F., Li, Z., Zhang, X., Xu, Y., He, J. (2024). Self-cleaning and multi-active sites amphoteric composite sponges: Efficient removal, selective adsorption and photocatalyst substrates of dyes. *Chemical Engineering Journal*, 494, 152865.

[25] Al-Fiydh, M.N., Najm, H.F., Karam, F.F., Baqir, S.J. (2024). Thermodynamics, kinetic study and equilibrium isotherm analysis of cationic dye adsorption by ternary composite. *Results in Chemistry*, 10, 101680.

[26] Jinnah, S.N.H.M.A., Ali, U.F.Md., Gopinath, S.C.B., Ibrahim, N., Ahmad, R., Zuki, F. M. (2024). Oil palm waste-derived reduced graphene oxide (rGO) for dynamic adsorption of dye in a fixed-bed system. *Desalination and Water Treatment*, 317, 100019.

[27] Wang, Y., Fang, L.P., Zhang, H.Y., Ren, J.J., Liang, T., Lv, X.B., Cheng, C.J., Yu, H.R. (2024). Efficient adsorption of cationic dyes by a novel honeycomb-like porous hydrogel with ultrahigh mechanical property. *International Journal of Biological Macromolecules*, XX, 134457.

[28] Jianhua, Y., Wang, Y., Liu, Z., Li, Y., Yang, H., Xu, Z.L. (2020). High efficient dye removal with hydrolyzed ethanolamine-Polyacrylonitrile UF membrane: rejection of anionic dye and selective adsorption of cationic dye. *Chemosphere,* 259,127390.